

Seeing Beyond Haze: Generative Nighttime Image Dehazing

Beibei Lin¹ Stephen Lin² Robby Tan¹

¹National University of Singapore, ²Microsoft Research Asia

beibei.lin@u.nus.edu, stevelin@microsoft.com, robbi.tan@nus.edu.sg



Figure 1. Qualitative results from NightDeFog’20 [56], NightEnhance’23 [21], SFSNiD’24 [7] and our method on real-world data. Our method not only reduces dense haze and strong glow effects but also infers missing background details and content in severely degraded regions.

Abstract

Nighttime image dehazing is particularly challenging when dense haze and intense glow severely degrade or completely obscure background information. Existing methods often encounter difficulties due to insufficient background priors and limited generative ability, both essential for handling such conditions. In this paper, we introduce *BeyondHaze*, a generative nighttime dehazing method that not only significantly reduces haze and glow effects but also infers background information in regions where it may be absent. Our approach is developed on two main ideas: gaining strong

background priors by adapting image diffusion models to the nighttime dehazing problem, and enhancing generative ability for haze- and glow-obscured scene areas through guided training. Task-specific nighttime dehazing knowledge is distilled into an image diffusion model in a manner that preserves its capacity to generate clean images. The diffusion model is additionally trained on image pairs designed to improve its ability to generate background details and content that are missing in the input image due to haze effects. Since generative models are susceptible to hallucinations, we develop our framework to allow user control over the generative level, balancing visual realism and factual accu-

racy. Experiments on real-world images demonstrate that *BeyondHaze* effectively restores visibility in dense nighttime haze.

1. Introduction

The degradation of nighttime imagery due to haze presents a formidable challenge, as the combination of low light conditions and atmospheric particles can significantly obscure scene details. Haze induces scattering and absorption of light, which not only reduces visibility but also creates glows around light sources that conceal the background. The resulting loss of visual information makes it difficult to accurately restore the original scene.

To address this problem, existing supervised nighttime dehazing methods (e.g., [4, 8, 9, 65]) rely primarily on synthetic datasets for training. However, the considerable domain gap between real-world and synthetic degradations—especially in cases of severe haze and glow—limits the effectiveness of their learned background priors. Semi-supervised nighttime dehazing methods (e.g., [7, 21, 56]) combine unlabeled real data with synthetic paired data for training, but their limited background priors and supervision lead to suboptimal performance. In addition, previous methods lack the generative ability to infer background content in regions completely obscured by dense haze or intense glow. As shown in Figure 1, such methods underperform in areas heavily degraded or entirely blocked due to haze.

In this paper, we introduce *BeyondHaze*, a generative nighttime dehazing method that not only enhances the visibility of scenes affected by haze or glow but also generatively infers background details in regions where the original information is missing. *BeyondHaze* is built upon two ideas: harnessing the power of image diffusion models to generate clean images by adapting them with dehazing knowledge, and strengthening their generative ability to produce haze-obscured background content through guided training.

We first pretrain a dehazing model by applying haze and its associated light effects to clear nighttime images and then training the model to restore the original images. This process enables the model to learn robust background priors. After acquiring these priors, the dehazing model generates initial dehazed images and their corresponding confidence maps from real-world haze images. The before-and-after image pairs with confidence maps are then used to fine-tune a pretrained text-to-image diffusion model equipped with LoRA [18], where only the LoRA parameters are updated during training. This approach allows our diffusion model, which possesses strong built-in world priors, to learn from real hazy images and develop generative dehazing capabilities.

To enhance the model’s ability to generate missing background details and occluded scene content due to haze, we

introduce two additional elements into our framework: a detail enhancement model and a severe degradation model. The detail enhancement model generates training pairs by employing super-resolution on the initial dehazed images from the pretrained dehazing model. Meanwhile, the severe degradation model applies strong haze and glow effects on clear nighttime images to produce training pairs that contain substantial obscuration and occlusion. These two types of training pairs are used to fine-tune our diffusion model, enabling it to create fine-scale details and infer missing backgrounds in heavily degraded areas.

Since these training pairs are used for re-creating background information that may be absent in hazy nighttime images, there is a potential to introduce hallucinations. Conversely, omitting these pairs may lead to less visually appealing results but helps to maintain factual accuracy. Our framework is thus designed to give users control over the generative level, allowing them to balance realism and authenticity based on their preferences. We implement this by combining specific text prompts with these training pairs and enabling users to control the generative level of the outputs through prompt selection.

As shown in Figure 1, our method not only reduces dense haze and strong glow effects but also infers missing backgrounds in severely degraded regions. Though the generated details and content may not exactly match those of the actual scene, high-quality generative output nevertheless remains important, as it improves visibility and overall image quality, especially in regions where precise background recovery is not possible. This approach yields more visually realistic predictions, which is particularly valuable for image editing applications. Moreover, by adjusting text prompts, we can control the level of generative inference.

Experimental results on real-world datasets demonstrate that *BeyondHaze* achieves significant performance improvements. Notably, our method achieves a MUSIQ score of 65.79 and a ClipIQA score of 0.6774, surpassing existing nighttime image dehazing methods by 27.4% in MUSIQ and 8.9% in ClipIQA. The main contributions of this work are as follows:

- We introduce generative dehazing priors, where knowledge from a pretrained dehazing model is transferred to a pretrained image diffusion model. This integration equips the diffusion model with both dehazing and generative capabilities.
- The generative ability of the diffusion model is improved for nighttime dehazing via training pairs produced by our detail enhancement model and severe degradation model.
- Control over the generative level of the output is made possible through the association of specific text prompts with the training pairs.
- Both qualitative and quantitative results demonstrate that *BeyondHaze* significantly improves the quality of real-

world nighttime haze images. Experimental results show that it not only suppresses degradation factors like haze and glow but also enhances overall image quality.

2. Related Work

Nighttime Image Dehazing Traditional image dehazing methods [3, 11, 15, 37, 49] address haze effects by estimating transmission maps and atmospheric light. However, these methods struggle with nighttime haze images, as the lower signal-to-noise ratio of nighttime images significantly affects the accuracy of transmission map and atmospheric light estimation. Existing daytime image dehazing methods [5, 6, 10, 13, 14, 19, 25–30, 34, 35, 41–44, 46, 47, 55, 58–60, 62, 66, 67] can be retrained on nighttime haze datasets. However, current nighttime haze datasets are synthetic, and models trained on them struggle to handle real-world haze due to the significant domain gap between real and synthetic degradations.

Existing nighttime image dehazing methods can be roughly divided into two categories: optimization-based and learning-based. The optimization-based dehazing methods [1, 2, 36, 40, 50, 52, 63, 64] utilize the atmospheric scattering model or a novel imaging model to reduce nighttime haze effects. However, nighttime haze images are also influenced by other complex factors, such as noise and glow effects, which significantly affect the accuracy of these models.

Learning-based nighttime image dehazing methods [21, 24, 56, 65] utilize paired synthetic data or unpaired real-world data to train neural networks. However, there is a significant domain gap between real-world and synthetic degradations that lead to inaccuracies when handling real-world haze images. Unsupervised and semi-supervised nighttime image dehazing methods [7, 21, 31, 56] primarily use unpaired data or pseudo ground truths for training. However, unpaired data lacks accurate pixel-level supervision, and pseudo ground truths often do not accurately represent areas with severe degradation due to the limitations of teacher models. Furthermore, these methods face challenges in recovering substantially obscured regions due to haze or low-light conditions because the true signal in these areas is much smaller than the degradation. To mitigate this issue, we utilize large-scale generative models, such as text-to-image diffusion models, to enhance visibility in nighttime haze images. By leveraging the strong generative capabilities of these models, our method is better equipped to handle haze effects, particularly in dense haze regions and extreme low-light conditions.

Diffusion Models for Restoration Diffusion models [17] have achieved remarkable success in various image restoration tasks, including deraining [32, 33], desnowing [38], and removing raindrops [22]. However, their generaliza-

tion ability is often constrained by the quality of training datasets. For nighttime image dehazing, the lack of real-world paired training data poses a significant challenge. Our work addresses this issue by utilizing different types of training data that target different aspects of nighttime dehazing, where each aspect is treated using reliable data for the corresponding sub-problem (*i.e.*, training pairs for dehazing without recovery of missing background information from a state-of-the-art dehazing model trained on real nighttime haze images, training pairs for detail enhancement by a pre-trained super-resolution model applied to dehazed images, and training pairs for missing background generation by a severe degradation model that obscures real-world image regions that would be heavily impacted by haze).

3. Proposed Method: BeyondHaze

Figure 2 illustrates the overall pipeline of *BeyondHaze*, which is based on generative dehazing priors and controllable generative dehazing. The generative dehazing priors are learned by distilling the knowledge of a pre-trained dehazing model into an image diffusion model with LoRA. Background detail and content generation are learned through training data from a detail enhancement model and a severe degradation model, where the generative level of the output is regulated by text prompts.

3.1. Generative Dehazing Priors

Our pre-trained dehazing model is a vision transformer [16] trained with severe augmentations [31], where clear images are intentionally degraded with light effects and noise. This forces the model to learn robust background priors, enabling it to infer clear scene information despite the degraded input.

Once the pre-trained dehazing model is obtained, we use it to generate initial dehazed images from real-world hazy nighttime images. These image pairs are then used to train our diffusion model, enabling it to progressively acquire task-specific dehazing knowledge while preserving its inherent generative properties. We refer to these integrated priors within the diffusion model as generative dehazing priors. Optimizing a large-scale diffusion model is, however, computationally expensive and risks degrading its generative properties. To address this, we employ LoRA [18], updating only its parameters during training. This preserves the model’s generative properties while incorporating dehazing capabilities.

Given a set of real nighttime haze images $\{\mathbf{x}_i^{\text{rh}} \mid i = 1, 2, \dots, N^{\text{rh}}\}$, where \mathbf{x}_i^{rh} denotes the i -th haze image and N^{rh} represents the total number of haze images, our pre-trained nighttime dehazing model, parameterized by w_{DH} , generates initial dehazed images, formulated as:

$$\mathbf{y}_i^{\text{rh}} = f_n(\mathbf{x}_i^{\text{rh}}; w_{\text{DH}}), \quad (1)$$

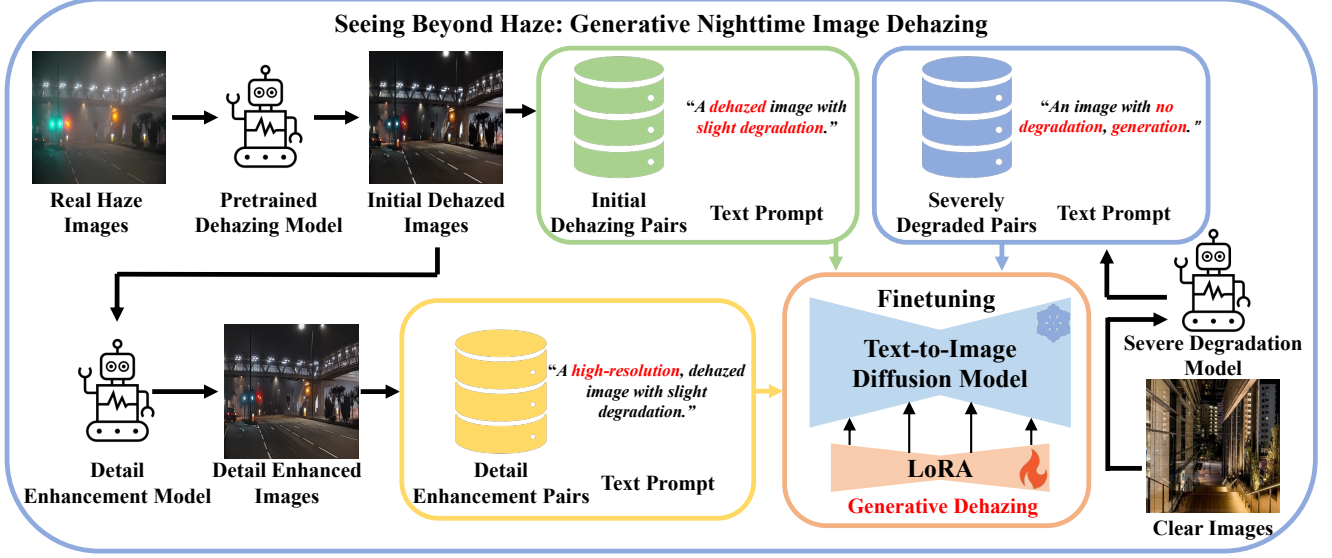


Figure 2. Our approach integrates dehazing priors with generative capabilities to enhance nighttime image dehazing. We first pretrain a dehazing model using augmentations that simulate noise and light effects in hazy night scenes. The knowledge from this dehazing model is then distilled into a pretrained image diffusion model with LoRA. Additional training pairs are generated by two supplementary models: a detail enhancement model that applies super-resolution to initial dehazed images, and a severe degradation model which produces substantially obscured images from real-world clear images. These training pairs, combined with customized text prompts, are used to fine-tune the diffusion model and enable controllable generative dehazing.

where \mathbf{y}_i^{rh} represents the initial dehazed images for the haze image \mathbf{x}_i^{rh} , and $f_n(x; w)$ denotes the inference process.

We additionally generate confidence maps \mathbf{m}_i^{rh} through overlapping sampling. A sliding window is applied to sample overlapping regions from the input \mathbf{x}_i^{rh} , such that each pixel receives multiple predictions, and the variance of these predictions is used to compute the confidence map \mathbf{m}_i^{rh} . The image pairs (i.e., real input images and their corresponding dehazed images) along with the confidence maps form a dataset $\mathbf{D}_{\text{ID}} = \{(\mathbf{x}_i^{\text{rh}}, \mathbf{y}_i^{\text{rh}}, \mathbf{m}_i^{\text{rh}})\}_{i=1}^{N^{\text{rh}}}$, which is used to fine-tune our diffusion model.

To learn dehazing priors while preserving the generative capabilities of the pre-trained diffusion model, we add a LoRA module, w_{LoRA} , to the diffusion model parameterized by w_{sd} . During training, w_{sd} remains fixed, and only w_{LoRA} is updated. We also inject a customized prompt t_{ID} during training to indicate that the training pairs represent initial dehazed images generated by our dehazing model. The diffusion model loss for these training pairs is formulated as:

$$\mathcal{L}_{\text{id}} = \frac{1}{B} \sum_{j=1}^B \mathbb{E}_{t, \epsilon} \left[\left\| \mathbf{m}_j^{\text{rh}} \cdot (\epsilon - \epsilon_{\theta}(\mathbf{y}_j^{\text{rh}}(t), t, t_{\text{ID}}, \mathbf{x}_j^{\text{rh}})) \right\|_2^2 \right], \quad (2)$$

where \mathcal{L}_{id} denotes the diffusion loss, and B is the batch size. Here, $\epsilon_{\theta}(\mathbf{y}_j^{\text{rh}}(t), t, t_{\text{ID}}, \mathbf{x}_j^{\text{rh}})$ is the predicted noise from the diffusion model with LoRA, parameterized by w_{sd} and w_{LoRA} , respectively. $\mathbf{y}_j^{\text{rh}}(t)$ is the target image at time step

t , while t , t_{ID} , and \mathbf{x}_j^{rh} represent the conditioning inputs for the pre-trained diffusion model. During training, the target image \mathbf{y}_j^{rh} and conditioning inputs \mathbf{x}_j^{rh} are encoded into latent features via a VAE encoder. For simplicity, this step is omitted in our equation.

Fine-tuning our diffusion model on the initial dehazing pairs enables it to acquire dehazing capabilities while preserving its generative capacity through the use of LoRA. During inference, the fine-tuned diffusion model, guided by a text prompt, enhances the visibility of real hazy images.

3.2. Controllable Generative Dehazing

Our diffusion model with generative dehazing priors is designed to remove the visual appearance of haze and refine regions prone to artifacts. To strengthen its ability to reconstruct background details lost due to the lower signal-to-noise ratio from low light conditions and haze, and to synthesize background regions missing due to strong degradation and glows, we incorporate a detail enhancement model and a severe degradation model to produce training pairs, as depicted in Figure 2. Through certain prompts, the generative level of the model can be controlled by the user.

Detail Enhancement Model The detail enhancement model employs image super-resolution to improve the fine-scale visual quality of the initial dehazed images generated by the pre-trained dehazing model. Since generative super-resolution methods are susceptible to hallucinating details,

we include a customized text prompt together with the training pairs to enable user control.

Given a lower-quality initial dehazed image \mathbf{y}_i^{rh} , the detail enhancement model produces a higher-quality counterpart \mathbf{y}_i^{hq} . Processing all initial dehazed images in \mathbf{D}_{ID} yields a detail enhancement dataset $\mathbf{D}_{\text{DE}} = \{(\mathbf{x}_i^{\text{rh}}, \mathbf{y}_i^{\text{hq}}, \mathbf{m}_i^{\text{rh}})\}_{i=1}^{N^{\text{rh}}}$. Similar to the training of generative dehazing priors, we include a text prompt t_{DE} with these training pairs to signify the detail enhancement.

The detail enhancement pairs are added to the initial dehazing pairs for diffusion model training. Incorporating the text prompts allows the model to learn generative-level attributes that can be selected by the user. The diffusion model loss for detail enhancement pairs is formulated as:

$$\mathcal{L}_{\text{de}} = \frac{1}{B} \sum_{j=1}^B \mathbb{E}_{t, \epsilon} \left[\left\| \mathbf{m}_j^{\text{rh}} \cdot (\epsilon - \epsilon_{\theta}(\mathbf{y}_j^{\text{hq}}(t), t, t_{\text{DE}}, \mathbf{x}_j^{\text{rh}})) \right\|_2^2 \right]. \quad (3)$$

In each training batch, \mathcal{L}_{id} and \mathcal{L}_{de} share the same real-world haze samples \mathbf{x}^{rh} , effectively assisting the model in learning different generative levels.

Severe Degradation Model While the training data from our detail enhancement model can help the diffusion model learn to synthesize fine-scale details missing from the initial dehazed images, it does not help with recovering background regions occluded by dense haze or strong glow. To address this, we introduce a severe degradation model to produce training data for improving such generative capabilities in diffusion models. The degradation model severely degrades clear nighttime images by blending light effects and adding noise, creating a heavily augmented dataset, formulated as in [31]:

$$I = W_b * J + (1 - W_b) * L + \epsilon, \quad (4)$$

where I is the augmented image, J is the clear image, W_b is the blend weight map, L is the light map and ϵ is the noise. We define the severity of the augmentation S as:

$$S = 1 - \mathbb{E} \left[\frac{W_b \cdot J}{I} \right] \quad (5)$$

where $\mathbb{E}[\cdot]$ represents the mean over all spatial dimensions (height, width, and channels) and S defines the severity ratio. At high severity levels, strong glow or noise significantly obscures certain regions, simulating real-world scenarios where background details are heavily degraded or entirely lost. Training on such data compels our diffusion model to infer missing background content from severe augmentations, enhancing its generative capability for highly degraded areas. Additionally, it aids the diffusion model in learning the distribution of clear nighttime images, reducing potential artifacts introduced by the initial dehazing and detail enhancement training pairs.

Given clear nighttime images, we create a severe degradation dataset, defined as $\mathbf{D}_{\text{BS}} = \{(\mathbf{x}_i^{\text{rc}}, \mathbf{y}_i^{\text{rc}})\}_{i=1}^{N^{\text{rc}}}$ where \mathbf{x}_i^{rc} and \mathbf{y}_i^{rc} denote the i -th augmented and clear images, respectively, and N^{rc} represents the total number of paired samples. Like for the detail enhancement model, these pairs are accompanied by a customized prompt t_{BS} and added to the training set. The training loss is expressed as:

$$\mathcal{L}_{\text{bs}} = \frac{1}{B} \sum_{j=1}^B \mathbb{E}_{t, \epsilon} \left[\left\| \epsilon - \epsilon_{w_{\text{stu}}}(\mathbf{y}_j^{\text{rc}}(t), t, t_{\text{BS}}, \mathbf{x}_j^{\text{rc}}) \right\|_2^2 \right], \quad (6)$$

where \mathcal{L}_{bs} denotes the background synthesis loss for the severe degradation data.

Final Loss The final loss function is given by:

$$\mathcal{L}_{\text{all}} = \mathcal{L}_{\text{id}} + \mathcal{L}_{\text{de}} + \mathcal{L}_{\text{bs}}. \quad (7)$$

In summary, we distill the dehazing knowledge of a pre-trained dehazing model into a pretrained diffusion model using the initial dehazing loss \mathcal{L}_{id} . By finetuning only the LoRA parameters while freezing the rest of the diffusion model, it retains its generative capabilities while learning to dehaze. Furthermore, the diffusion model is trained to generate fine-scale details and missing background regions via the detail enhancement loss \mathcal{L}_{de} and background synthesis loss \mathcal{L}_{bs} . By associating specific prompts with the three types of training data, the user is able to choose whether or not to generate fine-scale details or background regions in the results.

4. Experiments

In our experiments, we test on a real-world nighttime dataset and use five no-reference image quality assessment metrics, namely MUSIQ [23], ManIQA [57], ClipIQA [51], HyperIQA [48], and TRES [12], to calculate the quality scores of the dehazed results.

RealNightHaze is a real-world nighttime haze dataset consisting of 440 images. These images are sourced from previous studies [21, 31, 65]. Due to the complex degradation factors in RealNightHaze, including haze, glow effects, extreme darkness, and noise, this dataset provides a comprehensive basis for evaluating the performance of existing methods.

4.1. Implementation Details

Generative Dehazing Priors Our generative dehazing priors are obtained from a pre-trained dehazing model and a pre-trained diffusion model. In this paper, the dehazing model is a transformer network [16] pre-trained with strong augmentations [31], while *Stable Diffusion* v2 serves as the large-scale pre-trained diffusion model. To preserve the generative capability of the pre-trained diffusion model, we

Metrics	Uformer CVPR'22	Restormer CVPR'22	DiT ICCV'23	NightDeFog ECCV'20	NightEnhance ACM MM'23	SFSNiD CVPR'24	Ours w/o Gen	Ours
MUSIQ	44.33	45.04	46.02	51.61	50.56	43.28	60.29	65.79
TRES	51.58	51.89	53.87	68.88	59.08	38.50	68.05	80.08
ClipIQA	0.3256	0.3762	0.4316	0.3743	0.3673	0.3672	0.6217	0.6774
HyperIQA	0.4035	0.4068	0.4122	0.4462	0.3981	0.2839	0.4831	0.6139
ManIQA	0.3050	0.3210	0.3311	0.3273	0.2879	0.2468	0.3690	0.4964

Table 1. Quantitative comparison on the RealNightHaze dataset (evaluated at 512×512 resolution). Five non-reference metrics, namely MUSIQ [23], TRES [12], ClipIQA [51], HyperIQA [48], and ManIQA [57], are used for evaluation. For all five metrics, higher values are better. NightDeFog [56], NightEnhance [21] and SFSNiD [7] are nighttime image dehazing methods, while the remaining methods are image restoration backbones. “w/o Gen” denotes that neither generative detail enhancement nor region synthesis are selected.

integrate a LoRA module [45]. The rank of the low-rank decomposition in LoRA is set to 8, with a 10% dropout applied to the LoRA layers. Additionally, the LoRA α parameter is set to 16 to control the scaling of the learned updates.

During training, we utilize the dehazing model to construct training pairs from real-world data. These pairs along with their text prompt are then used to fine-tune the diffusion model. The training batch size is set to 12, with a gradient accumulation step of 4 for stable training. The learning rate is set to 2×10^{-4} for the U-Net and 4×10^{-5} for the text encoder, with an input resolution of 512×512 . The total number of training steps is set to 10,000.

Controllable Generative Dehazing The generative capabilities of our diffusion model are enhanced by using training pairs from the detail enhancement and severe degradation models. During training, we utilize the detail enhancement model [20] to recover fine-scale details in the initial dehazed images obtained from the pre-trained dehazing model, resulting in the detail enhancement image pairs. Additionally, we adopt the degradation strategy described in Section 3.2 to generate training pairs for background synthesis, where the severity ratio S is approximately 98%. These paired datasets, along with their respective text prompts, are used to train our diffusion model. The customized text prompt for initial dehazing pairs t_{ID} is “A dehazed image with slight degradation.”, while the text prompt for detail enhancement pairs t_{DE} is “A high-detail, dehazed image with slight degradation.”. The prompt for background synthesis pairs t_{bs} is “An image with no degradation, generation.”. Since the only difference between the text prompts for initial-dehazing and detail enhancement pairs is the term “high-detail,” this distinction can be effectively learned by our diffusion model.

In each training batch, we sample paired data equally from the initial-dehazing, detail-enhancement, and background-synthesis pairs to ensure effective training. During inference, given a real-world nighttime haze image, we utilize the fine-tuned diffusion model to enhance its visibility.

With the text prompt “A high-detail, dehazed image with no degradation, generation”, our fine-tuned diffusion model produces highly generative dehazed results with synthesis of details and background content. The text prompt “A dehazed image with slight degradation” would instead lead to low-generative results that do not contain synthesized details or backgrounds, yielding greater factual accuracy but lower visual quality.

4.2. Quantitative Evaluation on RealNightHaze

We evaluate the performance of our *BeyondHaze* method on the RealNightHaze dataset, with experimental results presented in Table 1. We compare our method against several state-of-the-art techniques, including Uformer [54], Restormer [61], DiT [39], NightDeFog [56], NightEnhance [21], and SFSNiD [7]. Uformer, Restormer, and DiT are restoration backbones trained on synthetic datasets, while the remaining methods are specifically designed for nighttime image dehazing.

Table 1 shows that our *BeyondHaze* achieves notable improvements across all non-reference metrics. For models trained on synthetic datasets, such as Restormer and DiT, their MUSIQ scores remain around 45. In contrast, existing nighttime image dehazing methods, such as NightDeFog and NightEnhance, demonstrate greater effectiveness in enhancing visibility in hazy images. For example, NightDeFog achieves MUSIQ and TRES scores of 51.61 and 68.88, respectively. By comparison, our method achieves MUSIQ and TRES scores of 65.79 and 80.08, surpassing NightDeFog by 14.18 and 11.2 points, respectively.

4.3. Qualitative Evaluation on RealNightHaze

Figure 3 presents a qualitative comparison of various methods on real-world nighttime haze data. It can be observed that existing nighttime image dehazing methods often suffer from noise artifacts and tend to produce dark outputs. In contrast, our method effectively suppresses haze effects, enhancing overall image visibility. Moreover, we find that

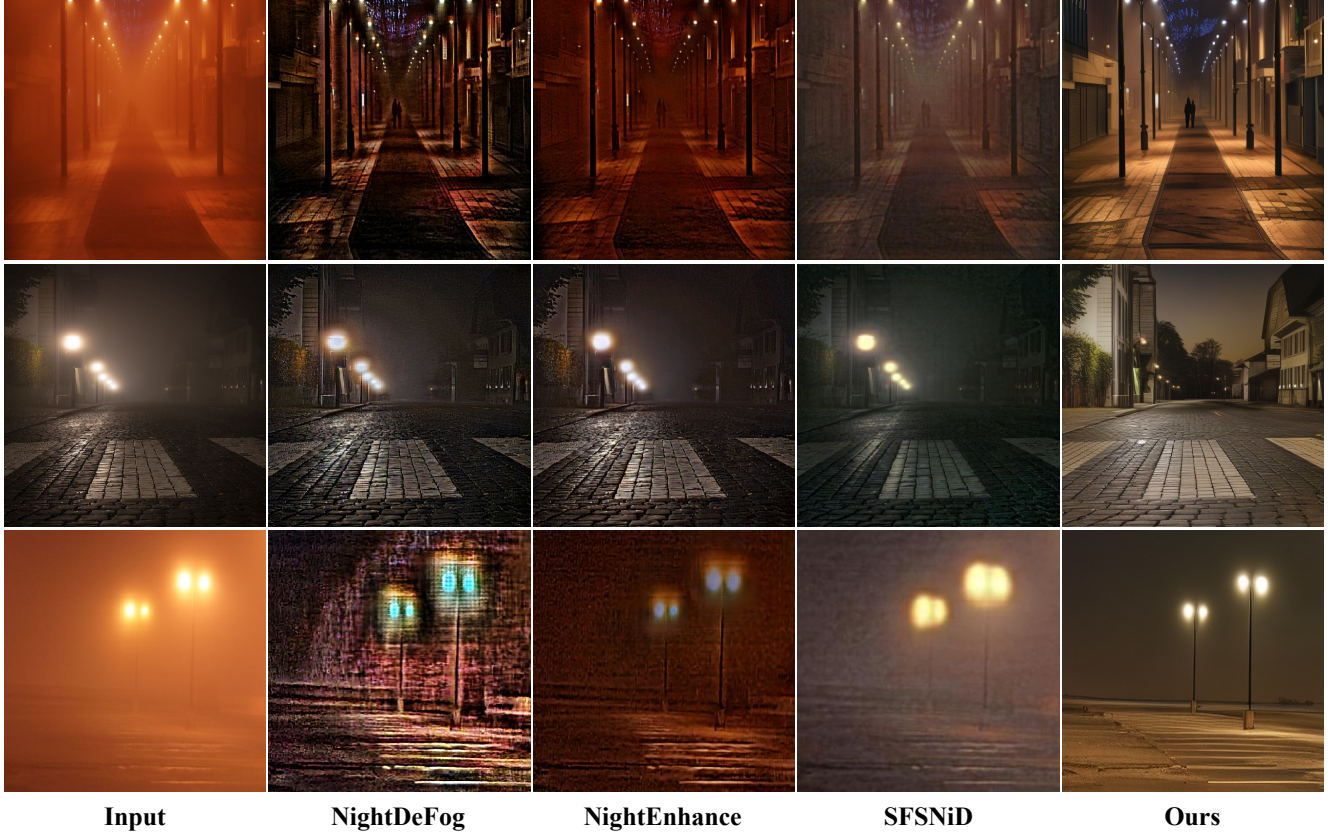


Figure 3. Qualitative results on the real-world haze dataset from NightDeFog’20 [56], NightEnhance’23 [21], SFSNiD’24 [7], and our method. Our method not only suppresses nighttime haze effects but also infers missing backgrounds in severely degraded regions.

existing nighttime image dehazing methods struggle to infer backgrounds in severely degraded regions, such as those affected by dense haze or strong glow. As shown in Figure 3 and Figure 4, these methods tend to generate black predictions in such regions. The primary reason is that information in these regions may be absent. Since these methods lack generative capabilities, they are unable to infer backgrounds, leading to inferior performance. In contrast, our *BeyondHaze* leverages strong priors from a pre-trained diffusion model to not only address haze effects but also infer backgrounds in regions entirely occluded by dense haze. As shown in Figure 3 and Figure 4, our method achieves significant performance improvements.

4.4. Ablation Studies

In this section, we perform ablation studies to validate our generative dehazing priors and controllable generative dehazing. The experimental results are presented in Table 2.

Analysis of the Generative Dehazing Priors Our pre-trained dehazing model achieves a MUSIQ score of 58.92, a TRES score of 63.83, and a ClipIQA score of 0.5290. In contrast, our finetuned diffusion model achieves a MUSIQ score of 60.29 and a ClipIQA score of 0.6217, surpassing the pre-

GDP	Supplementary Models		MUSIQ	TRES	ClipIQA
	Detail	Degradation			
×	×	×	58.92	63.83	0.5290
✓	×	×	60.29	68.05	0.6217
✓	✓	×	63.95	79.91	0.6570
✓	✓	✓	65.79	80.08	0.6774

Table 2. Ablation studies on real-world haze datasets. “GDP” denotes our generative dehazing priors. We use three non-reference metrics for evaluation: MUSIQ [23], TRES [12], and ClipIQA [51]. The scores in the first row are calculated from the results produced by our pre-trained dehazing model.

trained dehazing model by 1.37 in the MUSIQ score. This demonstrates that distilling knowledge from a pre-trained dehazing model to an image diffusion model leads to higher performance than the dehazing teacher model.

Analysis of Controllable Generative Dehazing Table 2 shows that our supplementary models designed for generative details and backgrounds lead to a substantial performance improvement. Including them yields a MUSIQ score of 65.79, outperforming the pre-trained dehazing model by

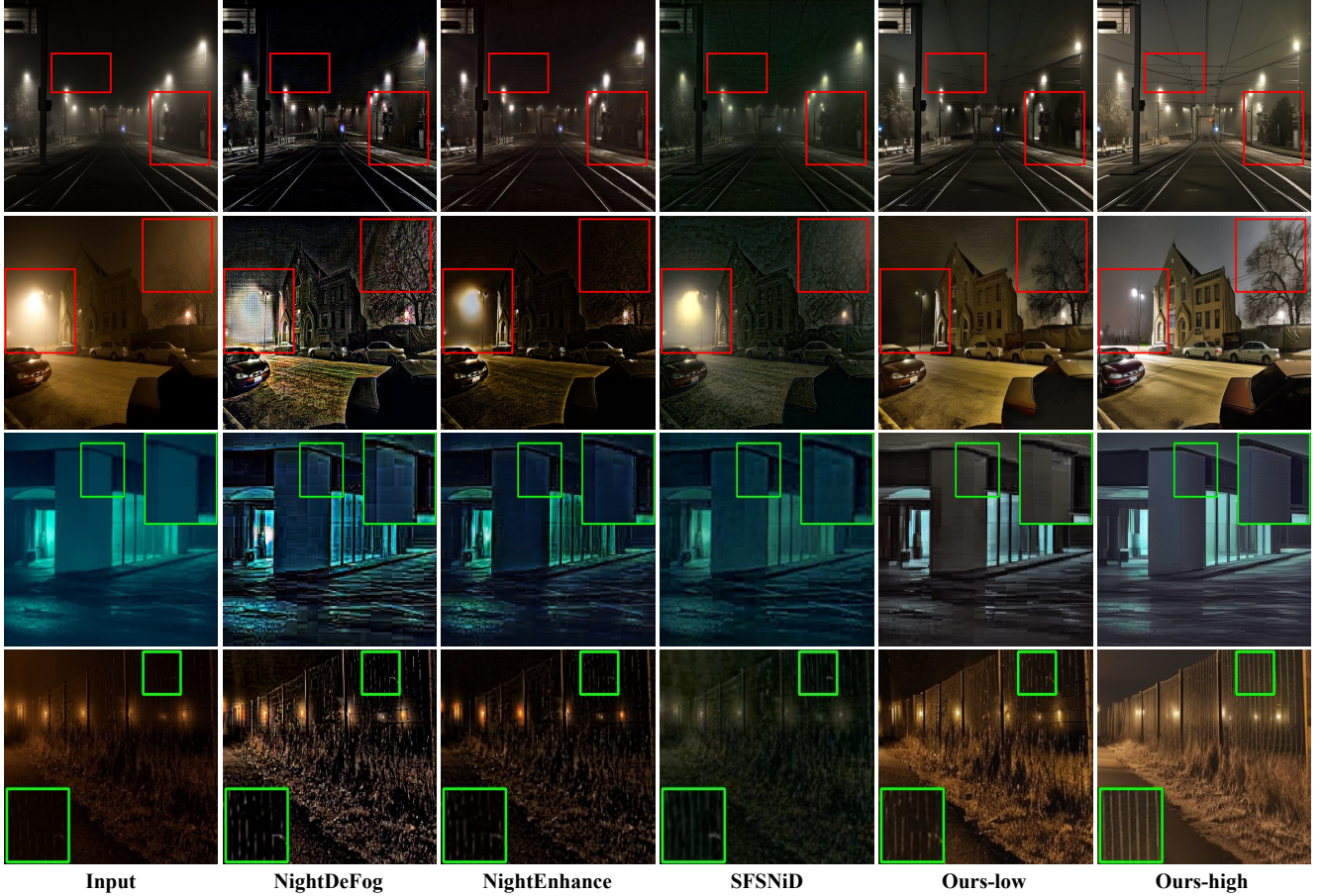


Figure 4. Qualitative results from NightDeFog’20 [56], NightEnhance’23 [21], SFSNiD’24 [7], and our method on real-world datasets. “Ours-low” refers to our low-generative results, which prioritize haze removal, while “Ours-high” refers to our high-generative results, allowing the network to infer details and backgrounds in severely degraded regions. The first two rows exhibit the ability of Ours-high to infer missing scene content, while the last two rows display fine-scale detail generation by Ours-high. Zoom in for better visualization.

6.87 points. This improvement demonstrates that the two models are effective at elevating the generative capabilities of the pre-trained diffusion model, resulting in superior performance.

Analysis of Different Generative Levels Using text prompts, our fine-tuned diffusion model can control the generative level of the outputs. The experimental results are shown in Figure 4. Our low-generative results, which prioritize haze removal, effectively mitigate haze effects but fail to infer background details and content in severely degraded regions. In contrast, our high-generative results enable the network to infer background details and content in these regions, significantly boosting visual quality.

5. Conclusion

This paper presents *BeyondHaze*, a novel generative approach for nighttime image dehazing that integrates dehazing priors with generative capabilities. We first pretrain a dehazing model using strong augmentations that simulate noise

and light effects in hazy night scenes, allowing the model to learn strong dehazing priors. This knowledge is then distilled into a diffusion model in a manner that preserves its generative capabilities. The generative power of the diffusion model for recovering fine-scale details and missing background regions in nighttime haze images is strengthened through training data from two additional models: a detail enhancement model and a severe degradation model. The detail enhancement model refines dehazed regions with lost details to produce detail enhancement training pairs, while the severe degradation model creates training pairs from clear images with severe augmentations to aid the diffusion model in learning to synthesize missing background areas. Customized text prompts are associated with these training pairs to allow users to control the level of generative dehazing in the outputs. Extensive experimental results on real-world nighttime datasets demonstrate that *BeyondHaze* achieves substantial improvements over other methods.

References

- [1] Cosmin Ancuti, Codruta O Ancuti, Christophe De Vleeschouwer, and Alan C Bovik. Night-time dehazing by fusion. In *2016 IEEE International Conference on Image Processing (ICIP)*, pages 2256–2260. IEEE, 2016. 3
- [2] Cosmin Ancuti, Codruta O Ancuti, Christophe De Vleeschouwer, and Alan C Bovik. Day and night-time dehazing by local airlight estimation. *IEEE Transactions on Image Processing*, 29:6264–6275, 2020. 3
- [3] Dana Berman, Tali Treibitz, and Shai Avidan. Single image dehazing using haze-lines. *IEEE transactions on pattern analysis and machine intelligence*, 42(3):720–734, 2018. 3
- [4] Silvano A Bernabel and Sos S Aghaian. Ndels: A novel approach for nighttime dehazing, low-light enhancement, and light suppression. *IEEE Transactions on Multimedia*, 2024. 2
- [5] Bolun Cai, Xiangmin Xu, Kui Jia, Chunmei Qing, and Dacheng Tao. Dehazenet: An end-to-end system for single image haze removal. *IEEE Transactions on Image Processing*, 25(11):5187–5198, 2016. 3
- [6] Zeyuan Chen, Yangchao Wang, Yang Yang, and Dong Liu. Psd: Principled synthetic-to-real dehazing guided by physical priors. In *Proceedings of the IEEE/CVF Conference on Computer Vision and Pattern Recognition*, pages 7180–7189, 2021. 3
- [7] Xiaofeng Cong, Jie Gui, Jing Zhang, Junming Hou, and Hao Shen. A semi-supervised nighttime dehazing baseline with spatial-frequency aware and realistic brightness constraint. In *Proceedings of the IEEE/CVF Conference on Computer Vision and Pattern Recognition*, pages 2631–2640, 2024. 1, 2, 3, 6, 7, 8, 12, 13, 14, 15, 16, 17, 18, 19, 20
- [8] Yuning Cui, Wenqi Ren, Xiaochun Cao, and Alois Knoll. Focal network for image restoration. In *Proceedings of the IEEE/CVF international conference on computer vision*, pages 13001–13011, 2023. 2
- [9] Yuning Cui, Wenqi Ren, and Alois Knoll. Omni-kernel network for image restoration. In *Proceedings of the AAAI Conference on Artificial Intelligence*, pages 1426–1434, 2024. 2
- [10] Hang Dong, Jinshan Pan, Lei Xiang, Zhe Hu, Xinyi Zhang, Fei Wang, and Ming-Hsuan Yang. Multi-scale boosted dehazing network with dense feature fusion. In *Proceedings of the IEEE/CVF conference on computer vision and pattern recognition*, pages 2157–2167, 2020. 3
- [11] Raanan Fattal. Single image dehazing. *ACM transactions on graphics (TOG)*, 27(3):1–9, 2008. 3
- [12] S Alireza Golestaneh, Saba Dadsetan, and Kris M Kitani. No-reference image quality assessment via transformers, relative ranking, and self-consistency. In *Proceedings of the IEEE/CVF Winter Conference on Applications of Computer Vision*, pages 1220–1230, 2022. 5, 6, 7
- [13] Alona Golts, Daniel Freedman, and Michael Elad. Unsupervised single image dehazing using dark channel prior loss. *IEEE Transactions on Image Processing*, 29:2692–2701, 2019. 3
- [14] Chun-Le Guo, Qixin Yan, Saeed Anwar, Runmin Cong, Wenqi Ren, and Chongyi Li. Image dehazing transformer with transmission-aware 3d position embedding. In *Proceedings of the IEEE/CVF Conference on Computer Vision and Pattern Recognition*, pages 5812–5820, 2022. 3
- [15] Kaiming He, Jian Sun, and Xiaoou Tang. Single image haze removal using dark channel prior. *IEEE transactions on pattern analysis and machine intelligence*, 33(12):2341–2353, 2011. 3
- [16] Kaiming He, Xinlei Chen, Saining Xie, Yanghao Li, Piotr Dollár, and Ross Girshick. Masked autoencoders are scalable vision learners. In *Proceedings of the IEEE/CVF conference on computer vision and pattern recognition*, pages 16000–16009, 2022. 3, 5, 12
- [17] Jonathan Ho, Ajay Jain, and Pieter Abbeel. Denoising diffusion probabilistic models. *Advances in neural information processing systems*, 33:6840–6851, 2020. 3
- [18] Edward J Hu, Yelong Shen, Phillip Wallis, Zeyuan Allen-Zhu, Yuanzhi Li, Shean Wang, Lu Wang, and Weizhu Chen. Lora: Low-rank adaptation of large language models. *arXiv preprint arXiv:2106.09685*, 2021. 2, 3
- [19] Lu-Yao Huang, Jia-Li Yin, Bo-Hao Chen, and Shao-Zhen Ye. Towards unsupervised single image dehazing with deep learning. In *2019 IEEE International Conference on Image Processing (ICIP)*, pages 2741–2745. IEEE, 2019. 3
- [20] JasperAI. Flux.1 – fluxcontrolnet upscaler, 2024. Software available from <https://github.com/jasperai/flux.1>. 6, 12
- [21] Yeying Jin, Beibei Lin, Wending Yan, Yuan Yuan, Wei Ye, and Robby T Tan. Enhancing visibility in nighttime haze images using guided apsf and gradient adaptive convolution. In *Proceedings of the 31st ACM International Conference on Multimedia*, pages 2446–2457, 2023. 1, 2, 3, 5, 6, 7, 8, 12, 13, 14, 15, 16, 17, 18, 19, 20
- [22] Yeying Jin, Xin Li, Jiadong Wang, Yan Zhang, and Malu Zhang. Raindrop clarity: A dual-focused dataset for day and night raindrop removal. In *European Conference on Computer Vision*, pages 1–17. Springer, 2024. 3
- [23] Junjie Ke, Qifei Wang, Yilin Wang, Peyman Milanfar, and Feng Yang. Musiq: Multi-scale image quality transformer. In *Proceedings of the IEEE/CVF International Conference on Computer Vision*, pages 5148–5157, 2021. 5, 6, 7
- [24] Shiba Kuanar, Dwarikanath Mahapatra, Monalisa Bilas, and KR Rao. Multi-path dilated convolution network for haze and glow removal in nighttime images. *The Visual Computer*, 38(3):1121–1134, 2022. 3
- [25] Boyi Li, Xiulian Peng, Zhangyang Wang, Jizheng Xu, and Dan Feng. Aod-net: All-in-one dehazing network. In *Proceedings of the IEEE international conference on computer vision*, pages 4770–4778, 2017. 3
- [26] Boyun Li, Yuanbiao Gou, Jerry Zitao Liu, Hongyuan Zhu, Joey Tianyi Zhou, and Xi Peng. Zero-shot image dehazing. *IEEE Transactions on Image Processing*, 29:8457–8466, 2020.
- [27] Boyun Li, Yuanbiao Gou, Shuhang Gu, Jerry Zitao Liu, Joey Tianyi Zhou, and Xi Peng. You only look yourself: Unsupervised and untrained single image dehazing neural network. *International Journal of Computer Vision*, 129(5):1754–1767, 2021.

- [28] Lerenhan Li, Yunlong Dong, Wenqi Ren, Jinshan Pan, Changxin Gao, Nong Sang, and Ming-Hsuan Yang. Semi-supervised image dehazing. *IEEE Transactions on Image Processing*, 29:2766–2779, 2019.
- [29] Runde Li, Jinshan Pan, Zechao Li, and Jinhui Tang. Single image dehazing via conditional generative adversarial network. In *Proceedings of the IEEE Conference on Computer Vision and Pattern Recognition*, pages 8202–8211, 2018.
- [30] Yi Li, Yi Chang, Yan Gao, Changfeng Yu, and Luxin Yan. Physically disentangled intra-and inter-domain adaptation for varicolored haze removal. In *Proceedings of the IEEE/CVF Conference on Computer Vision and Pattern Recognition*, pages 5841–5850, 2022. 3
- [31] Beibei Lin, Yeying Jin, Wending Yan, Wei Ye, Yuan Yuan, and Robby T Tan. Nighthaze: Nighttime image dehazing via self-prior learning. *arXiv preprint arXiv:2403.07408*, 2024. 3, 5, 12
- [32] Beibei Lin, Yeying Jin, Wending Yan, Wei Ye, Yuan Yuan, Shunli Zhang, and Robby T Tan. Nightrain: Nighttime video deraining via adaptive-rain-removal and adaptive-correction. In *Proceedings of the AAAI Conference on Artificial Intelligence*, pages 3378–3385, 2024. 3
- [33] Jiawei Liu, Qiang Wang, Huijie Fan, Yinong Wang, Yandong Tang, and Liangqiong Qu. Residual denoising diffusion models. In *Proceedings of the IEEE/CVF Conference on Computer Vision and Pattern Recognition*, pages 2773–2783, 2024. 3
- [34] Wei Liu, Xianxu Hou, Jiang Duan, and Guoping Qiu. End-to-end single image fog removal using enhanced cycle consistent adversarial networks. *IEEE Transactions on Image Processing*, 29:7819–7833, 2020. 3
- [35] Xiaohong Liu, Yongrui Ma, Zhihao Shi, and Jun Chen. Grid-dehazenet: Attention-based multi-scale network for image dehazing. In *Proceedings of the IEEE/CVF International Conference on Computer Vision*, pages 7314–7323, 2019. 3
- [36] Yun Liu, Zhongsheng Yan, Aimin Wu, Tian Ye, and Yuche Li. Nighttime image dehazing based on variational decomposition model. In *Proceedings of the IEEE/CVF Conference on Computer Vision and Pattern Recognition*, pages 640–649, 2022. 3
- [37] Gaofeng Meng, Ying Wang, Jiangyong Duan, Shiming Xiang, and Chunhong Pan. Efficient image dehazing with boundary constraint and contextual regularization. In *Proceedings of the IEEE international conference on computer vision*, pages 617–624, 2013. 3
- [38] Ozan Özdenizci and Robert Legenstein. Restoring vision in adverse weather conditions with patch-based denoising diffusion models. *IEEE Transactions on Pattern Analysis and Machine Intelligence*, 45(8):10346–10357, 2023. 3
- [39] William Peebles and Saining Xie. Scalable diffusion models with transformers. In *Proceedings of the IEEE/CVF International Conference on Computer Vision (ICCV)*, pages 4195–4205, 2023. 6, 12, 13, 14, 15, 16, 17, 18, 19, 20
- [40] Soo-Chang Pei and Tzu-Yen Lee. Nighttime haze removal using color transfer pre-processing and dark channel prior. In *2012 19th IEEE International conference on image processing*, pages 957–960. IEEE, 2012. 3
- [41] Xu Qin, Zhilin Wang, Yuanchao Bai, Xiaodong Xie, and Huizhu Jia. Ffa-net: Feature fusion attention network for single image dehazing. In *Proceedings of the AAAI Conference on Artificial Intelligence*, pages 11908–11915, 2020. 3
- [42] Yanyun Qu, Yizi Chen, Jingying Huang, and Yuan Xie. Enhanced pix2pix dehazing network. In *Proceedings of the IEEE Conference on Computer Vision and Pattern Recognition*, pages 8160–8168, 2019.
- [43] Wenqi Ren, Si Liu, Hua Zhang, Jinshan Pan, Xiaochun Cao, and Ming-Hsuan Yang. Single image dehazing via multi-scale convolutional neural networks. In *European conference on computer vision*, pages 154–169. Springer, 2016.
- [44] Wenqi Ren, Lin Ma, Jiawei Zhang, Jinshan Pan, Xiaochun Cao, Wei Liu, and Ming-Hsuan Yang. Gated fusion network for single image dehazing. In *Proceedings of the IEEE conference on computer vision and pattern recognition*, pages 3253–3261, 2018. 3
- [45] Nataniel Ruiz, Yuanzhen Li, Varun Jampani, Yael Pritch, Michael Rubinstein, and Kfir Aberman. Dreambooth: Fine tuning text-to-image diffusion models for subject-driven generation. In *Proceedings of the IEEE/CVF conference on computer vision and pattern recognition*, pages 22500–22510, 2023. 6
- [46] Yuanjie Shao, Lerenhan Li, Wenqi Ren, Changxin Gao, and Nong Sang. Domain adaptation for image dehazing. In *Proceedings of the IEEE/CVF Conference on Computer Vision and Pattern Recognition*, pages 2808–2817, 2020. 3
- [47] Yuda Song, Zhuqing He, Hui Qian, and Xin Du. Vision transformers for single image dehazing. *IEEE Transactions on Image Processing*, 32:1927–1941, 2023. 3
- [48] Shaolin Su, Qingsen Yan, Yu Zhu, Cheng Zhang, Xin Ge, Jinqiu Sun, and Yanning Zhang. Blindly assess image quality in the wild guided by a self-adaptive hyper network. In *Proceedings of the IEEE/CVF Conference on Computer Vision and Pattern Recognition*, pages 3667–3676, 2020. 5, 6
- [49] Robby T Tan. Visibility in bad weather from a single image. In *2008 IEEE conference on computer vision and pattern recognition*, pages 1–8. IEEE, 2008. 3
- [50] Qunfang Tang, Jie Yang, Xiangjian He, Wenjing Jia, Qingnian Zhang, and Haibo Liu. Nighttime image dehazing based on retinex and dark channel prior using taylor series expansion. *Computer Vision and Image Understanding*, 202:103086, 2021. 3
- [51] Jianyi Wang, Kelvin CK Chan, and Chen Change Loy. Exploring clip for assessing the look and feel of images. In *Proceedings of the AAAI Conference on Artificial Intelligence*, pages 2555–2563, 2023. 5, 6, 7
- [52] Wenhui Wang, Anna Wang, and Chen Liu. Variational single nighttime image haze removal with a gray haze-line prior. *IEEE Transactions on Image Processing*, 31:1349–1363, 2022. 3
- [53] Xintao Wang, Liangbin Xie, Chao Dong, and Ying Shan. Real-esrgan: Training real-world blind super-resolution with pure synthetic data. In *Proceedings of the IEEE/CVF international conference on computer vision*, pages 1905–1914, 2021. 12
- [54] Zhendong Wang, Xiaodong Cun, Jianmin Bao, Wengang Zhou, Jianzhuang Liu, and Houqiang Li. Uformer: A general

- u-shaped transformer for image restoration. In *CVPR*, 2022. 6
- [55] Haiyan Wu, Yanyun Qu, Shaohui Lin, Jian Zhou, Ruizhi Qiao, Zhizhong Zhang, Yuan Xie, and Lizhuang Ma. Contrastive learning for compact single image dehazing. In *Proceedings of the IEEE/CVF Conference on Computer Vision and Pattern Recognition*, pages 10551–10560, 2021. 3
- [56] Wending Yan, Robby T Tan, and Dengxin Dai. Night-time defogging using high-low frequency decomposition and grayscale-color networks. In *European Conference on Computer Vision*, pages 473–488. Springer, 2020. 1, 2, 3, 6, 7, 8, 12, 13, 14, 15, 16, 17, 18, 19, 20
- [57] Sidi Yang, Tianhe Wu, Shuwei Shi, Shanshan Lao, Yuan Gong, Mingdeng Cao, Jiahao Wang, and Yujiu Yang. Maniqa: Multi-dimension attention network for no-reference image quality assessment. In *Proceedings of the IEEE/CVF Conference on Computer Vision and Pattern Recognition*, pages 1191–1200, 2022. 5, 6
- [58] Yang Yang, Chaoyue Wang, Risheng Liu, Lin Zhang, Xiaojie Guo, and Dacheng Tao. Self-augmented unpaired image dehazing via density and depth decomposition. In *Proceedings of the IEEE/CVF Conference on Computer Vision and Pattern Recognition*, pages 2037–2046, 2022. 3
- [59] Tian Ye, Yunchen Zhang, Mingchao Jiang, Liang Chen, Yun Liu, Sixiang Chen, and Erkang Chen. Perceiving and modeling density for image dehazing. In *Computer Vision—ECCV 2022: 17th European Conference, Tel Aviv, Israel, October 23–27, 2022, Proceedings, Part XIX*, pages 130–145. Springer, 2022.
- [60] Hu Yu, Naishan Zheng, Man Zhou, Jie Huang, Zeyu Xiao, and Feng Zhao. Frequency and spatial dual guidance for image dehazing. In *Computer Vision—ECCV 2022: 17th European Conference, Tel Aviv, Israel, October 23–27, 2022, Proceedings, Part XIX*, pages 181–198. Springer, 2022. 3
- [61] Syed Waqas Zamir, Aditya Arora, Salman Khan, Munawar Hayat, Fahad Shahbaz Khan, and Ming-Hsuan Yang. Restormer: Efficient transformer for high-resolution image restoration. In *Proceedings of the IEEE/CVF conference on computer vision and pattern recognition*, pages 5728–5739, 2022. 6
- [62] He Zhang and Vishal M Patel. Densely connected pyramid dehazing network. In *Proceedings of the IEEE conference on computer vision and pattern recognition*, pages 3194–3203, 2018. 3
- [63] Jing Zhang, Yang Cao, and Zengfu Wang. Nighttime haze removal based on a new imaging model. pages 4557–4561. IEEE, 2014. 3
- [64] Jing Zhang, Yang Cao, Shuai Fang, Yu Kang, and Chang Wen Chen. Fast haze removal for nighttime image using maximum reflectance prior. In *Proceedings of the IEEE conference on computer vision and pattern recognition*, pages 7418–7426, 2017. 3
- [65] Jing Zhang, Yang Cao, Zheng-Jun Zha, and Dacheng Tao. Nighttime dehazing with a synthetic benchmark. In *Proceedings of the 28th ACM International Conference on Multimedia*, pages 2355–2363, 2020. 2, 3, 5
- [66] Shiyu Zhao, Lin Zhang, Ying Shen, and Yicong Zhou. Refinednet: A weakly supervised refinement framework for single image dehazing. *IEEE Transactions on Image Processing*, 30:3391–3404, 2021. 3
- [67] Zhuoran Zheng, Wenqi Ren, Xiaochun Cao, Xiaobin Hu, Tao Wang, Fenglong Song, and Xiuyi Jia. Ultra-high-definition image dehazing via multi-guided bilateral learning. In *2021 IEEE/CVF Conference on Computer Vision and Pattern Recognition (CVPR)*, pages 16180–16189. IEEE, 2021. 3

Supplementary Material

A. More Results on Real-world Datasets

In this section, we present additional real-world dehazing results comparing our *BeyondHaze* with state-of-the-art (SOTA) methods, including DiT’23 [39], NightDeFog’20 [56], NightEnhance’23 [21], and SFSNiD’24 [7]. DiT’23 serves as a general image restoration backbone trained on synthetic datasets, while the other SOTA methods are specialized nighttime image dehazing approaches trained using both labeled synthetic datasets and unlabeled real-world datasets. The experimental results are shown in Figs. S1 to S8. We can find that our *BeyondHaze* not only reduces dense haze and strong glow effects but also infers missing backgrounds in severely degraded regions.

B. Experimental Details

Our *BeyondHaze* is built upon on generative dehazing priors and controllable generative dehazing. We provide more training details as follow.

B.1. Generative Dehazing Priors

Our pre-trained dehazing model is a ViT-Large [16] architecture with 24 encoder layers and 8 decoder layers. During training, we initialize the model with pre-trained parameters from [16] and fine-tune it using augmentations from [31], where clear images are intentionally degraded with light effects and noise. This approach forces the model to learn robust background priors, enabling it to infer clear scene information despite degraded inputs.

During training, input images are randomly cropped to 224×224 . We set the total training steps to 20,000 and use a batch size of 128. The Adam optimizer is used with an initial learning rate of $1.5e-4$. During inference, we apply overlapping sampling to reconstruct high-resolution images, as ViT-Large only supports an input size of 224×224 . Specifically, a 224×224 sliding window is used to extract overlapping regions from high-resolution hazy inputs. The pre-trained dehazing model is then applied to restore these regions. Since each pixel receives multiple predictions, we average them to obtain the final dehazing results.

B.2. Controllable Generative Dehazing

We utilize the detail enhancement model [20] to recover fine-scale details in the initial dehazed images obtained from the pre-trained dehazing model. This model is built on FLUX.1 [20] and incorporates ControlNet, trained using the augmentation method from [53].

Our severe degradation model severely degrades clear nighttime images by blending light effects and adding noise,

creating a heavily augmented dataset, formulated as in [31]:

$$I = W_b * J + (1 - W_b) * L + \epsilon, \quad (8)$$

where I is the augmented image, J is the clear image, W_b is the blend weight map, L is the light map and ϵ is the noise. We define the severity of the augmentation S as:

$$S = 1 - \mathbb{E}\left[\frac{W_b \cdot J}{I}\right] \quad (9)$$

where $\mathbb{E}[\cdot]$ represents the mean over all spatial dimensions (height, width, and channels) and S defines the severity ratio.

Blend Weight Map W_b During training, for each input clear image J , we randomly sample a value from a uniform distribution (0.001, 0.1) to initialize a 512×512 map. Next, we randomly select eight 128×128 regions from this map. For each selected region, we randomly adjust its values within the range (0, 0.04). As a result, the blend weight map becomes non-uniform.

Light Map L We use real-world light maps for the augmentation, which is sourced from [31]. At each training step, we randomly select a light map for each clear image. Then, we select various regions and amplify their brightness using Gaussian kernels. The number of selected regions is between 1 and 10, and the size of Gaussian kernels ranges from 15 to 160.

Noise ϵ We introduce Gaussian noise to augment input images. We set W_n to 0.1, resulting in a noise range of (0, 0.03).

With these parameters, the severity S averages approximately 98% over all training steps. Note that the purpose of our severe augmentation model is to heavily degrade clear nighttime images, simulating real-world scenarios where background details are significantly degraded or entirely lost. It is not intended to perfectly simulate glow/haze effects or transmission maps. Therefore, Gaussian noise, the blend weight map, and the light map are sufficient as long as the augmentation remains severe.



(a) Input



(b) DiT [39]



(c) NightDeFog'20 [56]



(d) NightEnhance'23 [21]



(e) SFSNiD'24 [7]



(f) **Ours**

Figure S1. Qualitative results from DiT'23 [39], NightDeFog'20 [56], NightEnhance'23 [21], SFSNiD'24 [7], and our method, on the real-world dataset. Our method not only reduces dense haze and strong glow effects but also infers missing backgrounds in severely degraded regions. Zoom in for better visualization.



(a) Input



(b) DiT [39]



(c) NightDeFog'20 [56]



(d) NightEnhance'23 [21]



(e) SFSNiD'24 [7]



(f) **Ours**

Figure S2. Qualitative results from DiT'23 [39], NightDeFog'20 [56], NightEnhance'23 [21], SFSNiD'24 [7], and our method, on the real-world dataset. Our method not only reduces dense haze and strong glow effects but also infers missing backgrounds in severely degraded regions. Zoom in for better visualization.



(a) Input



(b) DiT [39]



(c) NightDeFog'20 [56]



(d) NightEnhance'23 [21]



(e) SFSNiD'24 [7]



(f) **Ours**

Figure S3. Qualitative results from DiT'23 [39], NightDeFog'20 [56], NightEnhance'23 [21], SFSNiD'24 [7], and our method, on the real-world dataset. Our method not only reduces dense haze and strong glow effects but also infers missing backgrounds in severely degraded regions. Zoom in for better visualization.



(a) Input



(b) DiT [39]



(c) NightDeFog'20 [56]



(d) NightEnhance'23 [21]



(e) SFSNiD'24 [7]



(f) **Ours**

Figure S4. Qualitative results from DiT'23 [39], NightDeFog'20 [56], NightEnhance'23 [21], SFSNiD'24 [7], and our method, on the real-world dataset. Our method not only reduces dense haze and strong glow effects but also infers missing backgrounds in severely degraded regions. Zoom in for better visualization.



(a) Input



(b) DiT [39]



(c) NightDeFog'20 [56]



(d) NightEnhance'23 [21]



(e) SFSNiD'24 [7]



(f) **Ours**

Figure S5. Qualitative results from DiT'23 [39], NightDeFog'20 [56], NightEnhance'23 [21], SFSNiD'24 [7], and our method, on the real-world dataset. Our method not only reduces dense haze and strong glow effects but also infers missing backgrounds in severely degraded regions. Zoom in for better visualization.



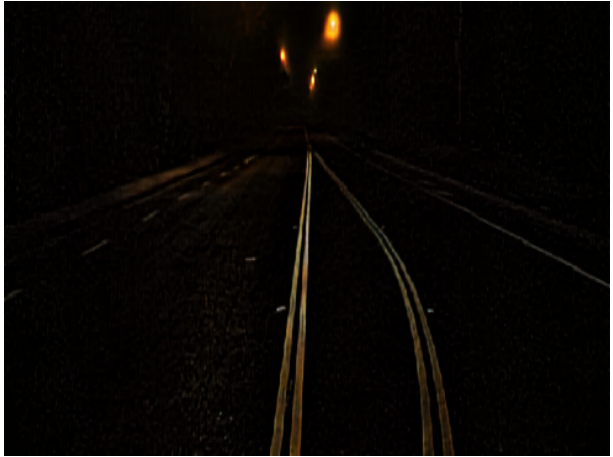
(a) Input



(b) DiT [39]



(c) NightDeFog'20 [56]



(d) NightEnhance'23 [21]



(e) SFSNiD'24 [7]



(f) **Ours**

Figure S6. Qualitative results from DiT'23 [39], NightDeFog'20 [56], NightEnhance'23 [21], SFSNiD'24 [7], and our method, on the real-world dataset. Our method not only reduces dense haze and strong glow effects but also infers missing backgrounds in severely degraded regions. Zoom in for better visualization.



(a) Input



(b) DiT [39]



(c) NightDeFog'20 [56]



(d) NightEnhance'23 [21]



(e) SFSNiD'24 [7]



(f) **Ours**

Figure S7. Qualitative results from DiT'23 [39], NightDeFog'20 [56], NightEnhance'23 [21], SFSNiD'24 [7], and our method, on the real-world dataset. Our method not only reduces dense haze and strong glow effects but also infers missing backgrounds in severely degraded regions. Zoom in for better visualization.



(a) Input



(b) DiT [39]



(c) NightDeFog'20 [56]



(d) NightEnhance'23 [21]



(e) SFSNiD'24 [7]



(f) Ours

Figure S8. Qualitative results from DiT'23 [39], NightDeFog'20 [56], NightEnhance'23 [21], SFSNiD'24 [7], and our method, on the real-world dataset. Our method not only reduces dense haze and strong glow effects but also infers missing backgrounds in severely degraded regions. Zoom in for better visualization.